Technote: Another Neural Net for first mass retrieval of water constituent concentrations from MERIS data

GKSS, H. Schiller

November 20, 2001

1 Introduction

This technote describes the latest development to realize the 'Case II water IMT–NN algorithm for the retrieval of water constituent concentrations from MERIS water leaving reflectance data' as described in [1].

The training data set for the NN's was derived from $23,400$ angular resolved spectra obtained from a modified `Hydrolight 3.0`. The water model used was that described in [2]. Parameters of this `Hydrolight` run are given in the appendix of [2].

For each of the $23,400$ angular resolved spectra 5 viewing geometries were randomly chosen

azimuth Φ: with equal chance from the interval limits as defined by the quads

zenith Θ_V: $\cos(\Theta_V)$ with constant probability from the range $[\cos(45°), 1.0]$.

The resulting points (spectra plus geometry and concentrations) were randomly assigned to the training and test data set with $112,021$ and $4,979$ points, respectively, and were used to generate the NN emulating the forward model as well as the NN emulating the inverse model. To train the NN emulating the inverse model the reflectances were modified according to the error model [3].

2 NN for retrieval of water constituent concentrations

The final NN to retrieve water constituent concentrations from MERIS water leaving reflectance data is a combination of three subNN's as shown in fig 1.

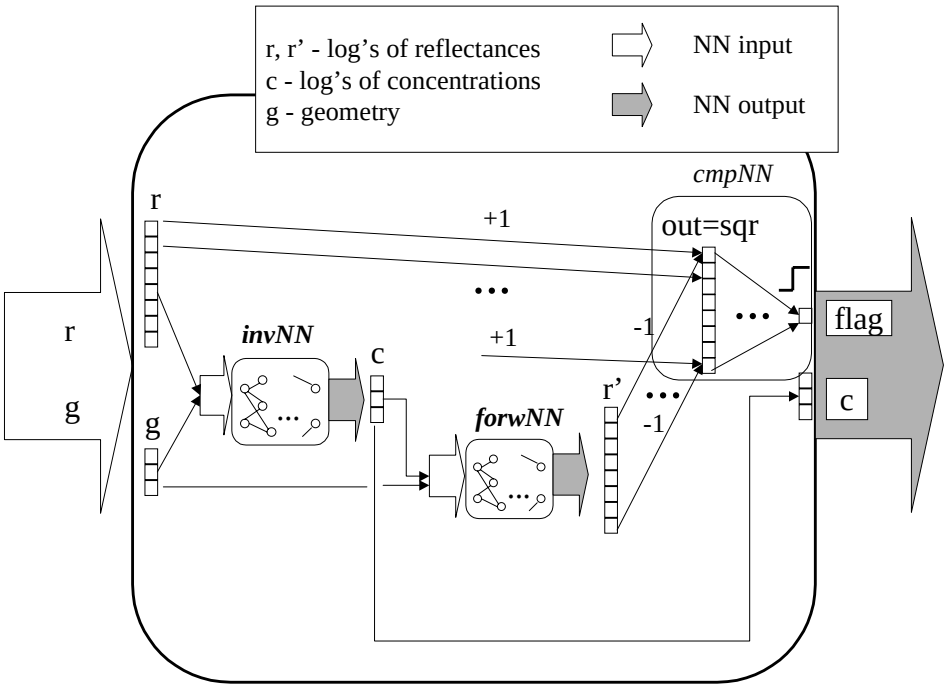

Figure 1: The combination of subNN's used to derive water constituent concentrations and the 'out of scope flag'

The task of the subNN's are:

`invNN` emulating the inverse model derives water constituent concentrations $\mathbf{c}$ from reflectances $\mathbf{r}$ and geometry information $\mathbf{g}$,

`forwNN` emulating the forward model derives reflectances $\mathbf{r}'$ from the concentrations (result of `invNN`) and the geometry $\mathbf{g}$,

`cmpNN` compares the measured reflectances $\mathbf{r}$ with the reflectance s$\mathbf{r}'$ from `forwNN`. Within the scope of the algorithm $\mathbf{r}$ and $\mathbf{r}'$ should agree. To large a disagreement signals measured reflectances outside the scope of the algorithm.

Thereby the combination of the subNN's retrieves water constituent concentrations **c** and an 'out of scope' flag from reflectances **r** and geometry information **g**.

2.1 The NN emulating the forward model

The NN emulating the forward model has 6 input neurons; their names and ranges are given in tab. 1.

Table 1: Names and ranges of input variables of `forwNN`

variable	*min*	*max*
Θ_{sun}	1.8	82.3
Θ_{view}	0.073	45.0
$\Delta\Phi$	0.0	180.0
log(tsm_g/m^3)	-2.44	4.36
log(chl_mg/m^3)	-0.82	3.27
log(a(gelb+part)442nm_1/m)	-5.27	1.49

The NN has two hidden layers with 15 and 20 neurons, respectively. The eight outout neurons produce the water leaving radiance reflectances in the MERIS channels from 412.3nm to 708.1nm. The *rms* of the (normalized) output neuron error is 0.013. Examples of comparisons of NN output with the corresponding model inputs from the test data set are shown in fig. 2.

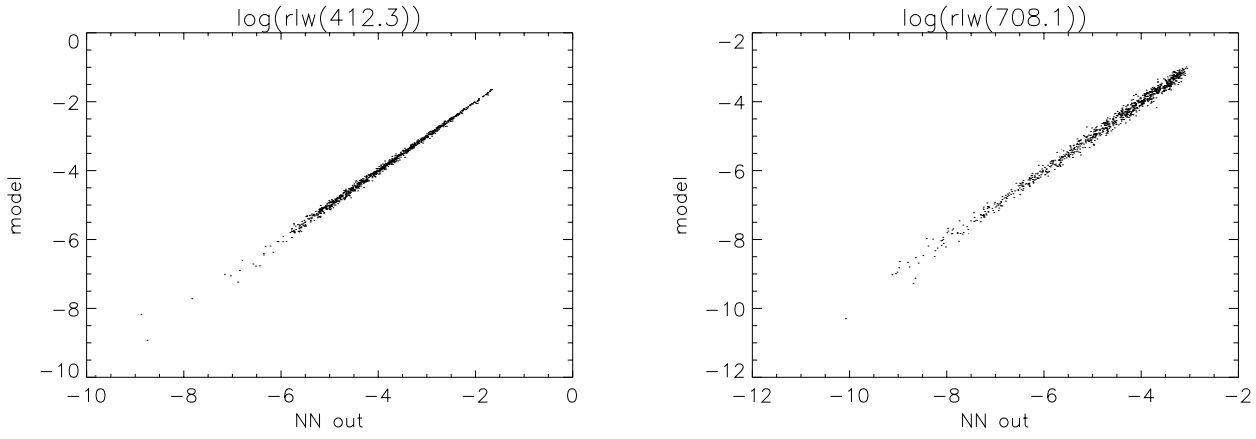

Figure 2: Examples of performance of `forwNN`

2.2 The NN emulating the inverse model

The NN emulating the inverse model has 11 input neurons; their names and ranges are given in tab. 2.

Table 2: Names and ranges of input variables of `invNN`

variable	*min*	*max*
Θ_{sun}	1.8	82.3
Θ_{view}	0.073	45.0
$\Delta\Phi$	0.0	180.0
log(rlw(412.3))	-9.96	-1.51
log(rlw(442.3))	-9.71	-1.51
log(rlw(489.7))	-7.76	-1.53
log(rlw(509.6))	-7.96	-1.62
log(rlw(559.5))	-7.54	-1.74
log(rlw(619.4))	-9.912	-2.27
log(rlw(664.3))	-10.20	-2.51
log(rlw(708.1))	-10.41	-2.84

The NN has three hidden layers with 60, 20 and 5 neurons, respectively. The three outout neurons produce the log's of water constituent concentrations. The *rms* of the (normalized) output neuron error is 0.043. Comparisons of NN output with the corresponding model inputs from the test data set are shown in fig. 3.

2.3 Out of dcope flag

Let d^2 the sum of the squared deviations calculated in the `cmpNN` part of the complete NN (see fig. 1). The problem is to find an appropriate value d^2_{cut} (position of the step function) to rise the flag if the agreement is bad. Until availability of real MERIS data there is no reasonable way to optimize the value of d^2_{cut}. Therefore we choose $d^2_{cut} = 0.6$ at the beginning since this cut accepts 98% of the spectra to which the error model was applied.

3 Discussion of scope and error budget of the algorithm

The plots in fig. 3 give an impression of the overall performance of the concentrations retrieval. Now the precision of the algorithm is not the same in

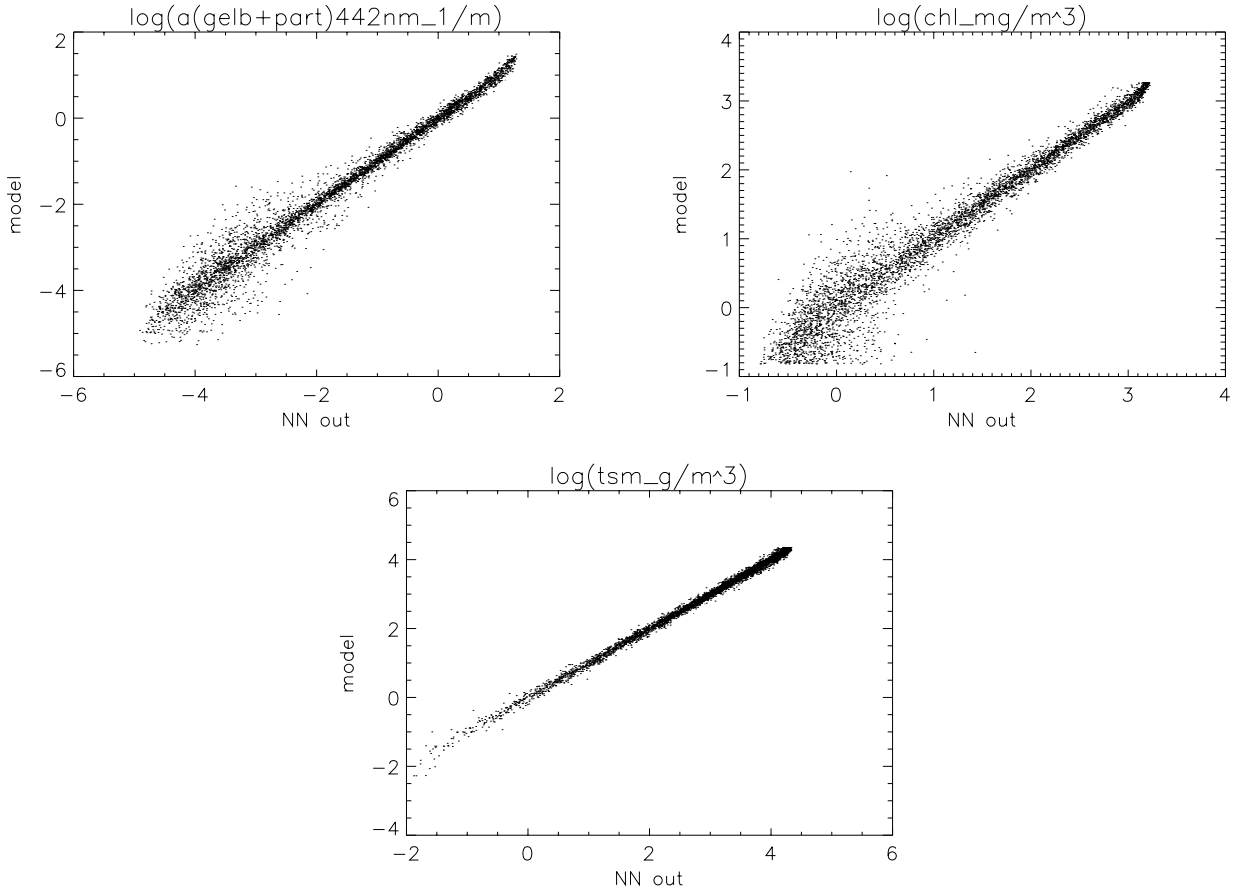

Figure 3: Performance of `invNN`

all the regions of the cuboid of concentrations. To make this statement more precise two more detailled evaluations were done. Both these evaluations used a data set which was generated in the same way (including the error model) as, but independently from, the NN training data set.

3.1 Looking at the extreme cases

To see the performance of the algorithm for the extreme cases we select from the cuboid of concentrations regions near edges of the cuboid, *i.e.* we restrict simultaneously two concentrations to be close to their respective limits and make no restriction to the third concentration as sketched in fig. 4.

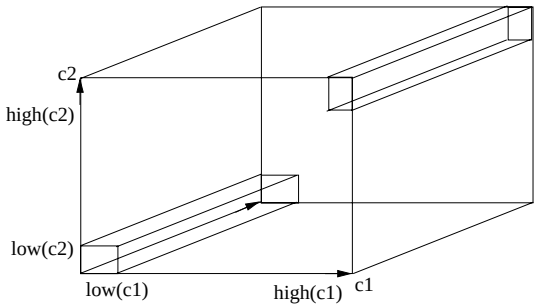

Figure 4: Illustration of restriction of concentrations to extreme cases

The low (high) values used for these cuts are listed in table 3.

Table 3: Values used to select concentrations close to cuboid edges

variable	*low*	*high*
tsm_g/m^3	0.7	70
chl_mg/m^3	0.6	19
a(gelb+part)442nm_1/m	0.01	2.5

Restriction of a(gelb+part)/tsm concentrations to the extreme cases results in the retrieval performance shown in fig. 5. There are no high chl concentrations if the other two concentrations are low by construction of the bio–optical model.

The chl retrieval has an acceptable error if the other concentrations are low, but is to high in the lower range if the other two concentrations are high. The a(gelb+part) retrieval is bad for low tsm concentrations.

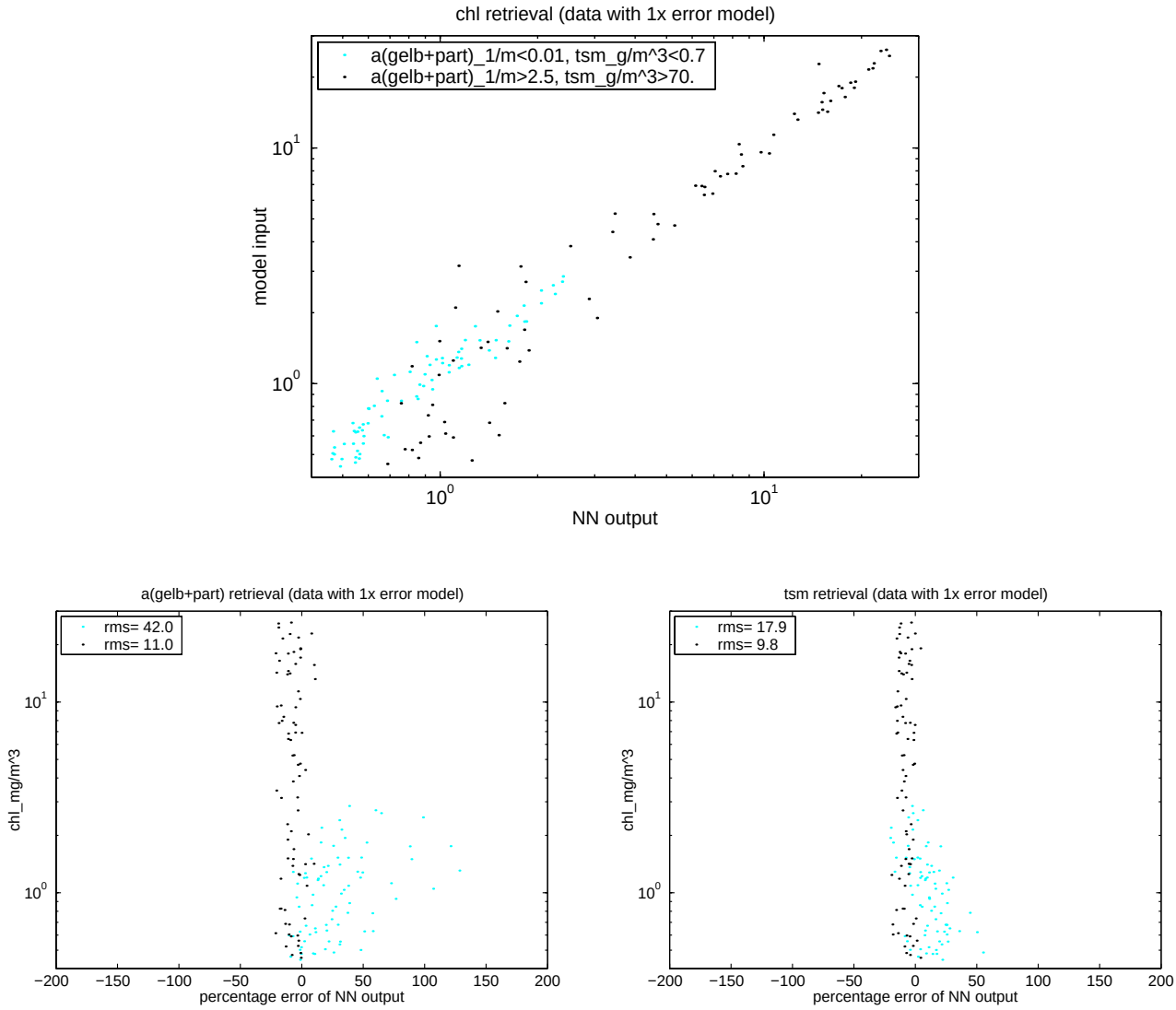

Figure 5: Performance of the NN for low (high) a(gelb+part)/tsm concentrations. The lower two plots show the percentage retrieval error for the two restricted variables.

Restriction of chl/tsm concentrations to the extreme cases results in the retrieval performance shown in fig. 6

Generally the a(gelb+part) retrieval is the most error prone. It becomes useless in its low concentration region if the other two concentrations are high.

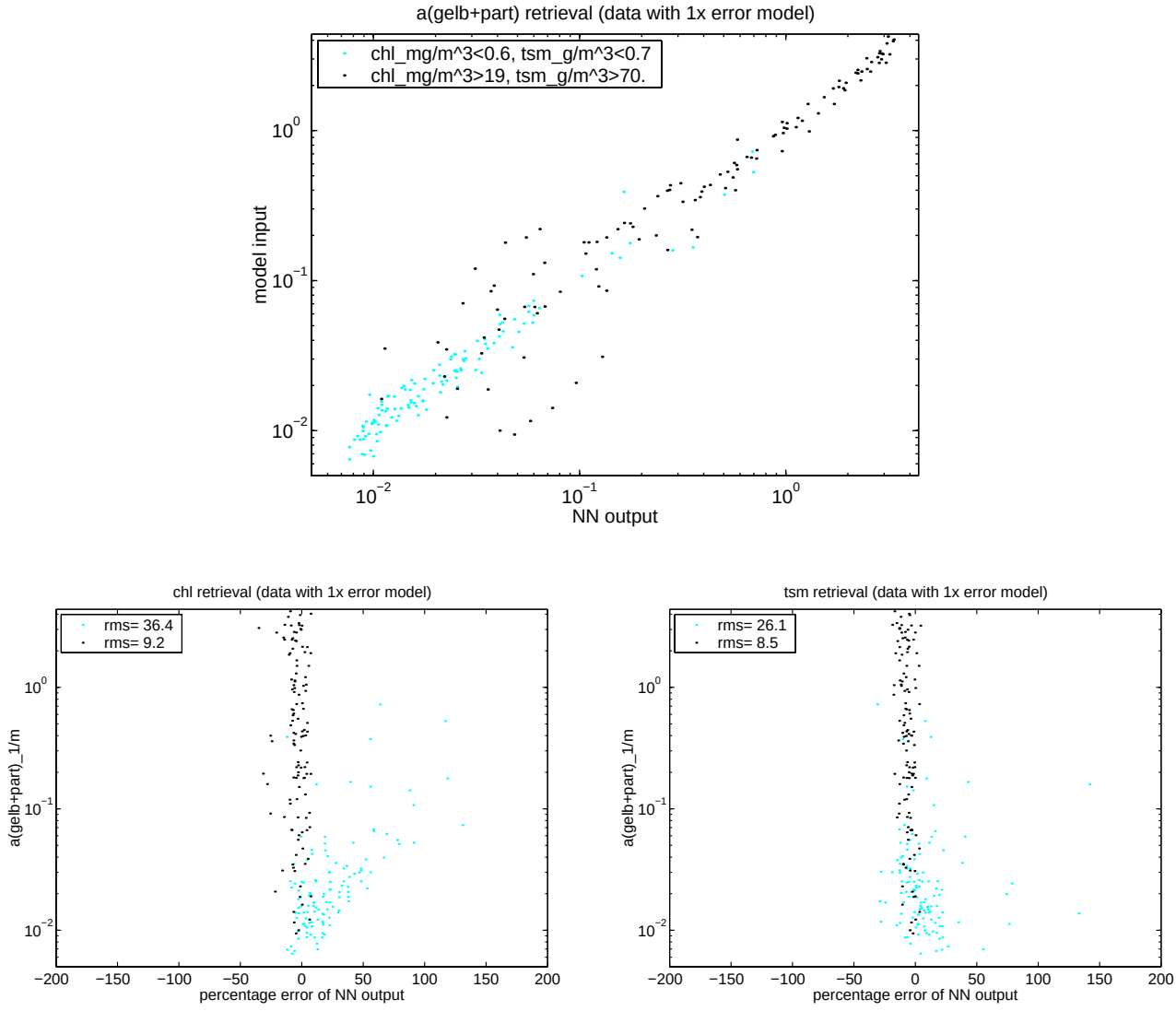

Figure 6: Performance of the NN for low (high) chl/tsm concentrations. The lower two plots show the percentage retrieval error for the two restricted variables.

Restriction of a(gelb+part)/chl concentrations to the extreme cases results in the retrieval performance shown in fig. 7. By construction of the bio–optical model there are no low tsm concentrations if both others are high.

The tsm concentration retrieval works well in all covered concentration regions.

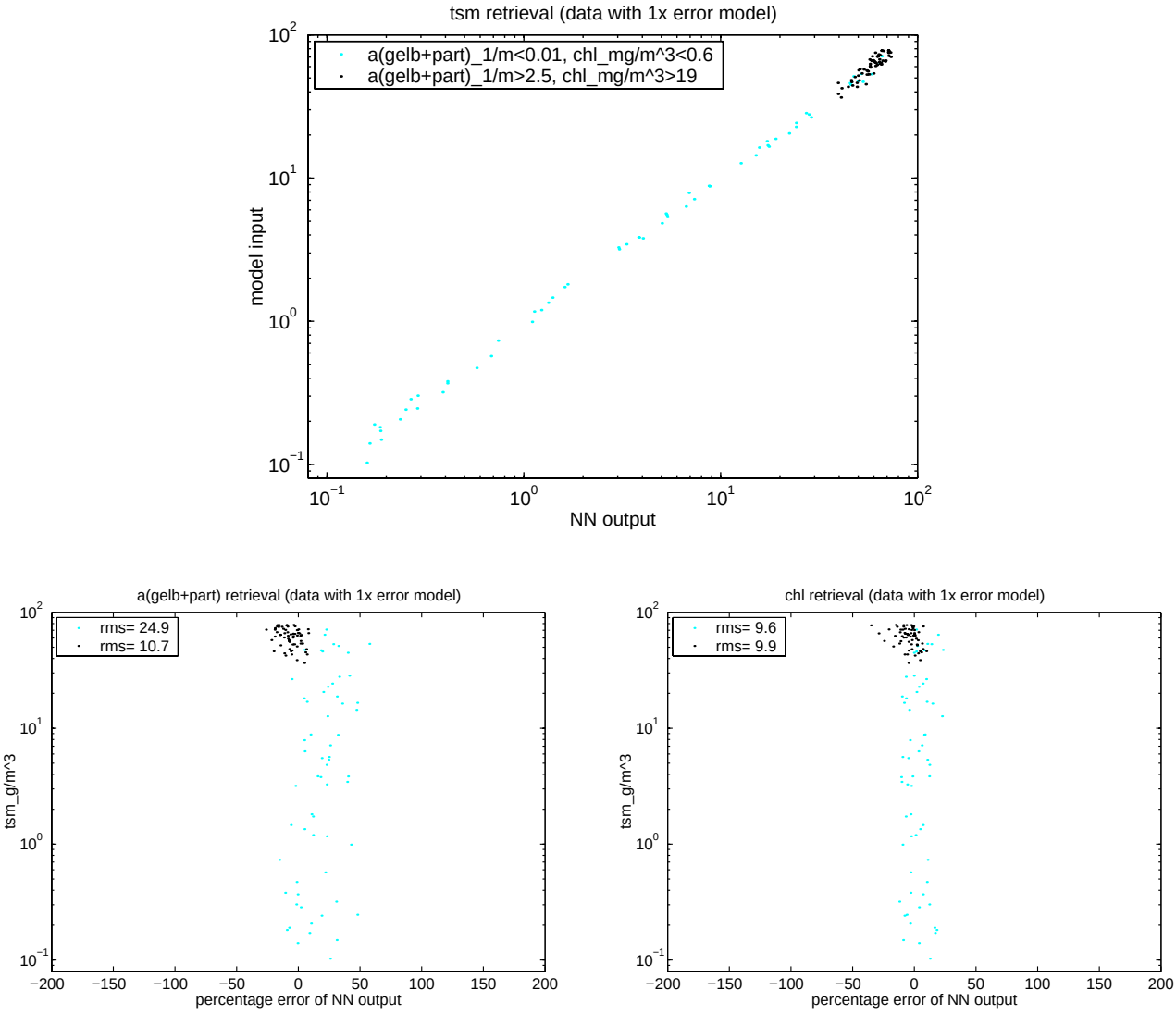

Figure 7: Performance of the NN for low (high) a(gelb+part)/chl concentrations. The lower two plots show the percentage retrieval error for the two restricted variables.

3.2 Splitting the concentrations cuboid

The concentrations cuboid was split into $27 = 3^3$ parts by defining for each concentration a 'low', 'medium' and 'high' range according to the limits listed in tab. 4. In fig. 8 the *rms* of percentage retrieval errors are shown. Within

Table 4: Values used to define 'low', 'medium' and 'high' concentration ranges

tsm_g/m^3	.09	...	.9	...	8.	...	80.
chl_mg/m^3	.44	...	1.7	...	7.	...	27.
a(gelb+part)442nm_1/m	.005	...	.05	...	.5	...	4.4

each of the nine subplots the first (leftmost) group of bars belongs to the 'low' chl concentration, the second to 'mediun' and the third to 'high' chl concentration. The same applies to the three columns which correspond to tsm concentrations and the three rows correspond to a(gelb+part) concentrations (lowest row $\sim$ lowest concentration). From fig. 8 we conclude with respect to retrieval performance:

tsm

- acceptable in all regions
- worst at small tsm and high a(gelb+part) concentration
- not influenced by chl concentration

chl

- becoming worse with rising a(gelb+part) concentration
- no retrieval possible when a(gelb+part) has high and tsm has 'low' or 'medium' concentration

a(gelb+part)

- at low concentrations becoming worse with rising chl as well as with rising tsm concentrations
- at low tsm concentration the error rises with rising a(gelb+part) concentration.

References

[1] Doerffer, R. and Schiller, H.: 'Pigment Index, Sediment and Gelbstoff Retrieval from directional water-leaving reflectances using inverse modelling technique', ATBB 2.12 in: MERIS Level 2 Algorithm Theoretical Basis Document. Doc. No. PO-TN-MEL-GS-0005 Issue 4 Rev. 1, 18. Feb. 2000

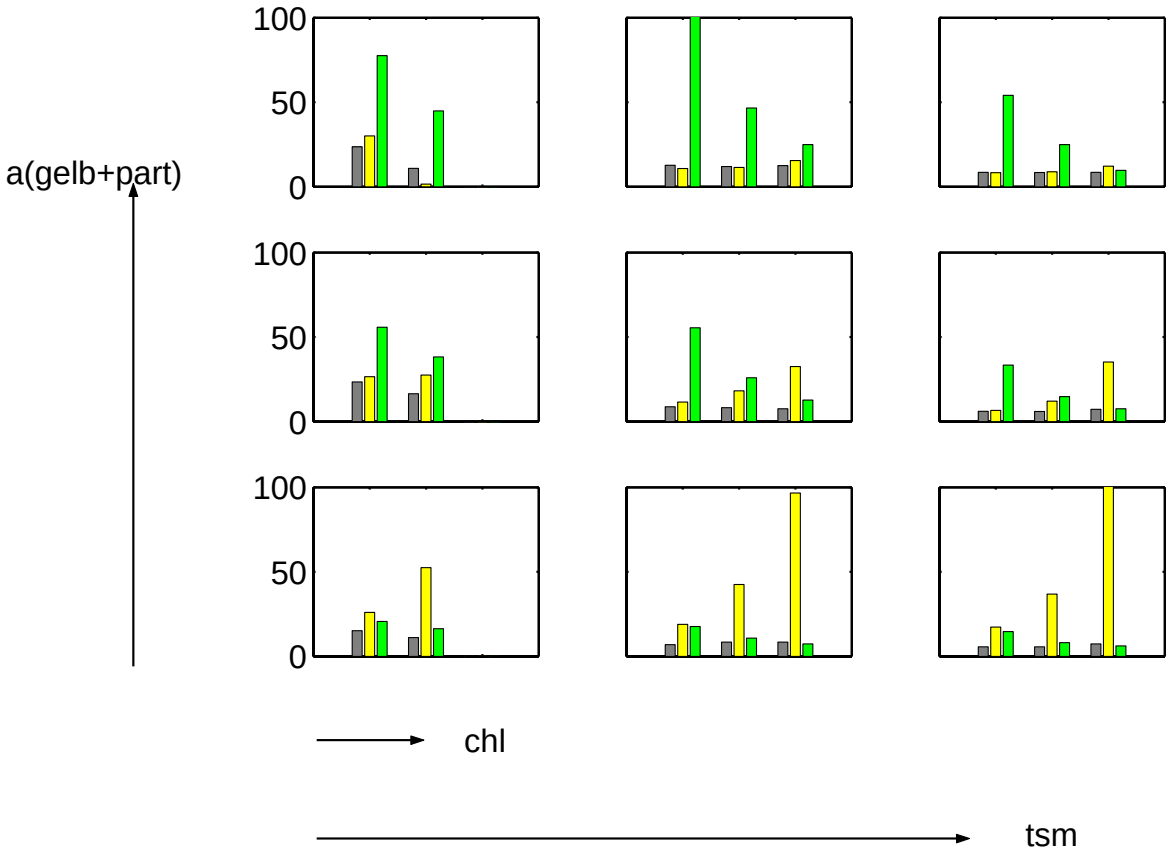

Figure 8: The *rms* of percentage retrieval error for tsm (grey), a(gelb+part) (yellow) and chl (green) are shown for different concentration regions as indicated by the arrows

[2] Roland Doerffer: 'Bio–optical component model of case II water for training of the (artificial) Neural Net algorithm for MERIS', Technote May 8th, 2001.

[3] Technical note: A simple reflectance error model above Case 2 waters', ACRI, (23/12/1999)